Babiskin AH and Smolke CD

SUPPLEMENTARY INFORMATION

Supplementary Figure 1 Plasmid map of pCS321, the Rnt1p hairpin characterization plasmid.

Supplementary Figure 2 Sequences illustrating the placement of the ΔTCT-4 aptamer within R31L-3B4Inv at multiple locations.

Supplementary Figure 3 The dose response curves of RS, RS-B03, RS-B05, and RS-B06 indicate that these synthetic BSB modules increase baseline expression relative to the original Rnt1p switch (RS).

Supplementary Table 1 Oligonucleotide template sequences for all switches built in this study.

Supplementary Table 2 The theoretical fold-change and dynamic range of all Rnt1p switches examined in this study as determined from experimentally measured baseline expression at 0 mM theophylline (*b*) and the theoretical maximal output (*M*) calculated by fitting the dose response data to the binding model.

Supplementary Table 3 The previously reported gene-regulatory activity of the synthetic BSB modules selected for use in this study in the context of the Rnt1p hairpin genetic control element (A02).

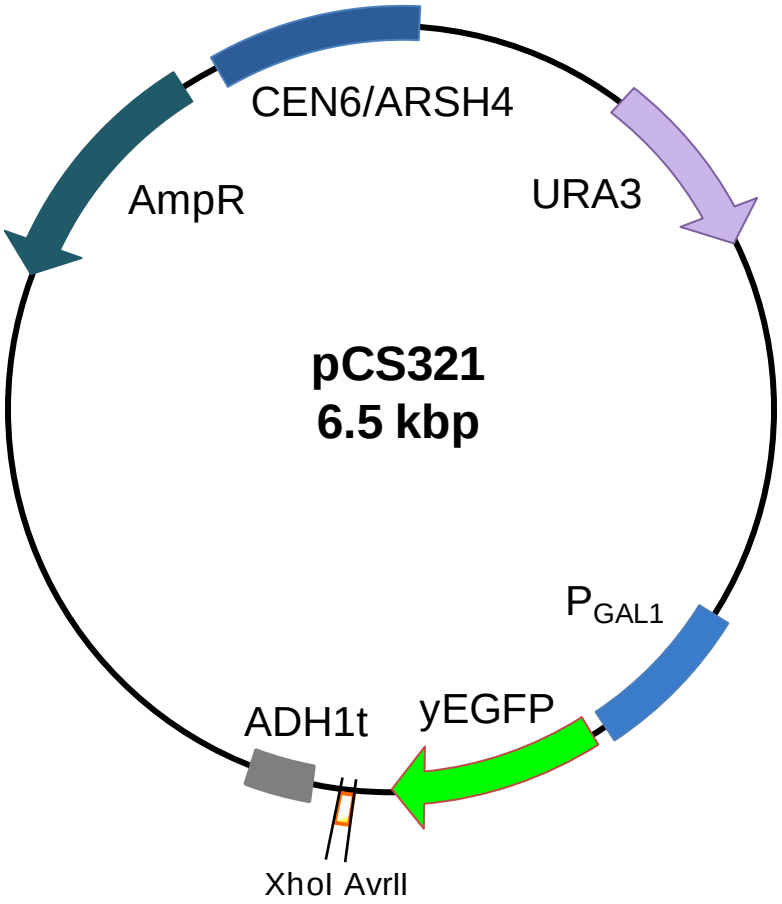

Supplementary Figure S1. Plasmid map of pCS321, the Rnt1p hairpin characterization plasmid.

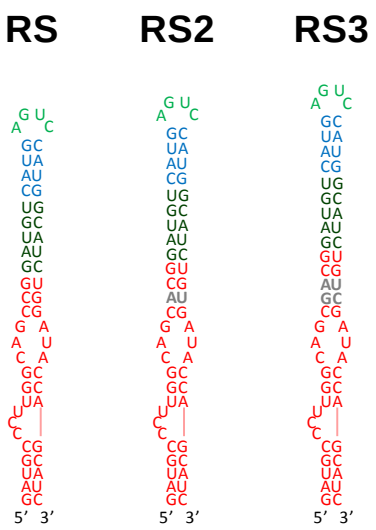

Supplementary Figure S2. Sequences illustrating the placement of the ΔTCT-4 aptamer within R31L-3B4Inv at multiple locations. RS2 and RS3 resulted in nonfunctional switches that were unresponsive to theophylline (data not shown), while RS was functional and utilized as the base Rnt1p switch design in this study. Gray lettering is used to indicate the nucleotides in RS2 and RS3 that differ from RS.

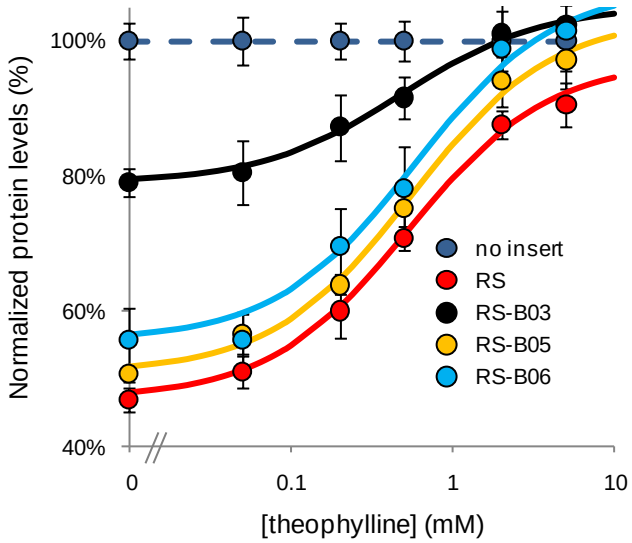

Supplementary Figure S3. The dose response curves of RS, RS-B03, RS-B05, and RS-B06 indicate that these synthetic BSB modules increase baseline expression relative to the original Rnt1p switch (RS). These switches exhibit a reduced fold-change relative to that exhibited by RS. Data are reported as indicated in Figure 1C. The model parameters for the curve fit are provided in Table I.

Supplementary Table 1. Oligonucleotide template sequences for all switches built in this study. The sequences of the indicated primers are provided in the Materials and Methods section.

switch	forward primer	reverse primer	template
SR	SR_fwd	SR_rev	AAACAAACTTGATGCCCTTGGCAGCCGGATGTCATGAGTC CATGGCATCTGGATACCAGCATCGTAAAAAGAAAAATAAA
SRN	SR_fwd	SR_rev	AAACAAACTTGATGCCCTTGGCAGCCGGATGTCATGCATC CATGGCATCTGGATACCAGCATCGTAAAAAGAAAAATAAA
SRnt	SRnt_fwd	SR_rev	AAACAAACTTGATGCCATTGGCAGCCGGATGTCATGAGTC CATGGCATCTGGATACCAGCATCGTAAAAAGAAAAATAAA
SR-theo2	SR-theo2_fwd	SR-theo2_rev	AAACAAACTTGGCCCTTGGCAGCCGGATGTCATGAGTCCA TGGCATCTGGATACCAGCCGTAAAAAGAAAAATAAA
SR-theo3	SR_fwd	SR_rev	AAACAAACTTGATGCCCTTGGCAGCACGATGTCATGAGTC CATGGCATCGTGATACCAGCATCGTAAAAAGAAAAATAAA
SR-B03	SR_fwd	SR_rev	AAACAAACTTGATGCCCTTGGCAGCCGGATGTTGAAAGTC TTCAGCATCTGGATACCAGCATCGTAAAAAGAAAAATAAA
SR-B05	SR_fwd	SR_rev	AAACAAACTTGATGCCCTTGGCAGCCGGATGTTGTAAGTC TACGGCATCTGGATACCAGCATCGTAAAAAGAAAAATAAA
SR-B06	SR_fwd	SR_rev	AAACAAACTTGATGCCCTTGGCAGCCGGATGTAATGAGTC CATTGCATCTGGATACCAGCATCGTAAAAAGAAAAATAAA
SR-B07	SR_fwd	SR_rev	AAACAAACTTGATGCCCTTGGCAGCCGGATGTTGTGAGTC CACAGCATCTGGATACCAGCATCGTAAAAAGAAAAATAAA
SR-B12	SR_fwd	SR_rev	AAACAAACTTGATGCCCTTGGCAGCCGGATGTAGTGAGTC CACTGCATCTGGATACCAGCATCGTAAAAAGAAAAATAAA
SRx2	SRx2_fwd	SRx2_rev	AAACAAACTTGATGCCCTTGGCAGCCGGATGTCATGAGTC CATGGCATCTGGATACCAGCATCGTAAAAAGAAAAATAAA
SRx3	SRx3_fwd	SRx3_rev	AAACAAACTTGATGCCCTTGGCAGCCGGATGTCATGAGTC CATGGCATCTGGATACCAGCATCGTAAAAAGAAAAATAAA
SR-B07x2	SRx2_fwd	SRx2_rev	AAACAAACTTGATGCCCTTGGCAGCCGGATGTTGTGAGTC CACAGCATCTGGATACCAGCATCGTAAAAAGAAAAATAAA
SR-B12x2	SRx2_fwd	SRx2_rev	AAACAAACTTGATGCCCTTGGCAGCCGGATGTAGTGAGTC CACTGCATCTGGATACCAGCATCGTAAAAAGAAAAATAAA
SR-theo3-B07	SR_fwd	SR_rev	AAACAAACTTGATGCCCTTGGCAGCACGATGTTGTGAGTC CACAGCATCGTGATACCAGCATCGTAAAAAGAAAAATAAA
SR-theo3-B12	SR_fwd	SR_rev	AAACAAACTTGATGCCCTTGGCAGCACGATGTAGTGAGTC CACTGCATCGTGATACCAGCATCGTAAAAAGAAAAATAAA

Supplementary Table 2. The theoretical fold-change and dynamic range of all Rnt1p switches examined in this study as determined from experimentally measured baseline expression at 0 mM theophylline (*b*) and the theoretical maximal output (*M*) calculated by fitting the dose response data to the binding model.

switch	b=Y(0mM)	M	theorectical fold-change	theorectical dynamic range
SR	47% ± 2%	97% ± 1%	2.07 ± 0.08	50% ± 2%
SR-theo2	52% ± 2%	94% ± 3%	1.79 ± 0.08	41% ± 3%
SR-theo3	42% ± 2%	101% ± 1%	2.40 ± 0.11	59% ± 2%
SR-B03	79% ± 4%	105% ± 1%	1.33 ± 0.07	26% ± 4%
SR-B05	51% ± 1%	104% ± 2%	2.04 ± 0.06	53% ± 2%
SR-B06	56% ± 5%	108% ± 3%	1.94 ± 0.17	52% ± 6%
SR-B07	44% ± 2%	112% ± 4%	2.56 ± 0.12	68% ± 4%
SR-B12	44% ± 2%	101% ± 2%	2.26 ± 0.11	56% ± 3%
SRx2	20% ± 1%	92% ± 0%	4.54 ± 0.16	71% ± 1%
SRx3	10% ± 0%	74% ± 1%	7.18 ± 0.32	64% ± 1%
SR-B07x2	16% ± 1%	89% ± 2%	5.42 ± 0.33	72% ± 2%
SR-B12x2	22% ± 0%	81% ± 2%	3.69 ± 0.10	59% ± 2%
SR-theo3-B07	37% ± 2%	103% ± 2%	2.79 ± 0.15	66% ± 3%
SR-theo3-B12	36% ± 1%	95% ± 2%	2.61 ± 0.11	59% ± 2%

Supplementary Table 3. The previously reported gene-regulatory activity of the synthetic BSB modules selected for use in this study in the context of the Rnt1p hairpin genetic control element (A02). The data is taken from previous work (A Babiskin and C Smolke, in preparation [b]).

substrate	Normalized protein levels (%)	Normalized transcript levels (%)
A02-B00	28% ± 1%	43% ± 8%
A02-B03	50% ± 2%	53% ± 5%
A02-B05	25% ± 0%	39% ± 3%
A02-B06	27% ± 2%	57% ± 2%
A02-B07	37% ± 3%	51% ± 3%
A02-B12	27% ± 2%	47% ± 5%